A NEW STACKING OPERATOR FOR CURVED SUBSURFACE STRUCTURES

C. Vanelle, B Kashtan, S. Dell, and D. Gajewski

email: *claudia.vanelle@zmaw.de*
keywords: *travelimes, multiparameter stacking, CRS*

ABSTRACT

Multiparameter stacking has become a standard tool for seismic reflection data processing. Different traveltime operators exist, whose accuracy depends on the offset and reflector curvature. We introduce a new, implicit stacking operator derived from evaluating Snell's law at a locally spherical interface. Comparison of the resulting traveltime surface with those obtained from the common reflection surface and multifocusing expressions confirm high accuracy and only minor dependence on the reflector curvature. The examples show that the new method performs well for the whole range of reflector curvatures from nearly planar reflectors to the diffraction limit.

INTRODUCTION

Over the past years, a number of multiparameter stacking operators have been introduced as an extension of the CMP stacking technique. Examples of such operators are the common reflection surface stack (CRS, Mueller, 1999), Multifocusing (MF, Gelchinksy et al., 1999), and the shifted hyperbola (de Bazelaire, 1988). These operators describe the traveltime surface for a reflected event in the short offset limit. The accuracy of the individual methods differs and depends not only on the considered offset but also on the reflector curvature.

In this work, we suggest a new stacking operator. It is derived from Snell's law for a spherical interface and leads to an implicit expression for the traveltime surface. Although the operator can be applied in an iterative fashion, we show in our examples that already a single iteration leads to higher accuracy than the CRS and MF expressions.

After a brief summary of the CRS and MF methods, we introduce a new implicit stacking operator (ISO) and examine its performance in comparison to CRS and MF.

COMMON REFLECTION SURFACE

The CRS stacking technique was introduced by Mueller (1999) to obtain a simulated zero offset section. The CRS stack can be considered as an extension of the classic CMP method, where stacking is carried out over offsets, while in the CRS technique the stack is applied over offsets and midpoints. This leads to a much larger number of contributing traces, and, thus, to a higher level of the signal to noise ratio.

Whereas the CMP operator is a hyperbola, the corresponding CRS operator is a traveltime surface of second order that includes the CMP operator as subset. Written in midpoint ($x_m = x_0 + \Delta x_m$) and half-offset (h) coordinates, the CRS operator for monotypic reflections in the two-dimensional zero-offset case

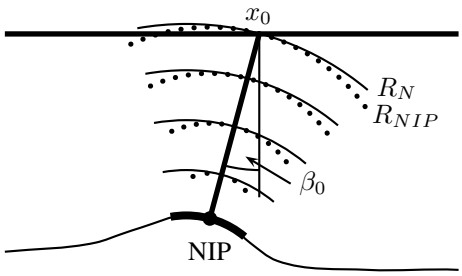

Figure 1: The meaning of the ZO-CRS parameters β_0, R_{NIP}, and R_N. NIP indicates the normal incidence point.

reads,

$$t^2(x_m,h) = \left[t_0 + \frac{2\sin\beta_0}{V_0}\,\Delta x_m\right]^2 + \frac{2\,t_0\,\cos^2\beta_0}{V_0}\left[\frac{\Delta x_m^2}{R_N} + \frac{h^2}{R_{NIP}}\right] \quad . \tag{1}$$

It contains three wave field attributes or parameters that describe physical properties of the one-way-process corresponding to the zero-offset situation, namely, the incidence or emergence angle β_0; the curvature K_{NIP} of a wave generated by a point source at the normal incidence point (NIP), the so-called NIP wave; and the curvature K_N of a wavefront generated by an exploding reflector element, the so-called normal wave. Furthermore, the velocity V_0 is that at the source and receiver. The meaning of the attributes is illustrated in Figure 1. The extension to 3D is straightforward (Müller, 2007).

The parameters are useful for a variety of applications like attribute-based time migration, determination of geometrical spreading, migration weights and apertures, and Fresnel zones (for an overview, see, e.g. Mann, 2002). More advanced applications that were recently introduced are NIP-wave tomography (Duveneck, 2004), multiple suppression (Dümmong and Gajewski, 2008), and data regularisation and prestack data enhancement (Dümmong et al., 2009).

MULTIFOCUSING

The multifocusing operator describes the traveltime of a reflected event in terms of the traveltime of a central ray and corrections applied at the source and receiver for a paraxial ray. This results in the double square root expression (e.g., Landa et al., 2010),

$$t(x_s,x_g) = \frac{1}{V_0}\sqrt{R_s^2 + 2\,R_s\Delta x_s\sin\beta_0 + \Delta x_s^2} + \frac{1}{V_0}\sqrt{R_g^2 + 2\,R_g\Delta x_g\sin\beta_0 + \Delta x_g^2} \quad , \tag{2}$$

with the source and receiver positions x_s and x_g, respectively, and $\Delta x_s = x_s - x_0$ and $\Delta x_g = x_g - x_0$. The quantities R_s and R_g are related to the radii of the N- and NIP-wave by

$$R_s = \frac{1+\sigma}{R_N^{-1} + \sigma\,R_{NIP}^{-1}} \quad \text{and} \quad R_g = \frac{1-\sigma}{R_N^{-1} - \sigma\,R_{NIP}^{-1}} \quad , \tag{3}$$

where σ is the so-called focusing parameter. For a detailed discussion of its meaning, please refer to Landa et al. (2010). If the reflector is locally plane, the focusing parameter can be expressed by

$$\sigma = \frac{\Delta x_s - \Delta x_g}{\Delta x_s + \Delta x_g + 2\,\dfrac{\Delta x_s\,\Delta x_g}{R_{NIP}}\sin\beta_0} \quad . \tag{4}$$

In a recently-published paper, Landa et al. (2010) state that the accuracy of multifocusing traveltimes can be enhanced by using the focusing parameter σ accordingly for a spherical reflector. However, the computation of the parameter σ even for the spherical case is not straightforward. Therefore, we have restricted our traveltime comparison to planar multifocusing, i.e., using the planar focusing parameter given by (4).

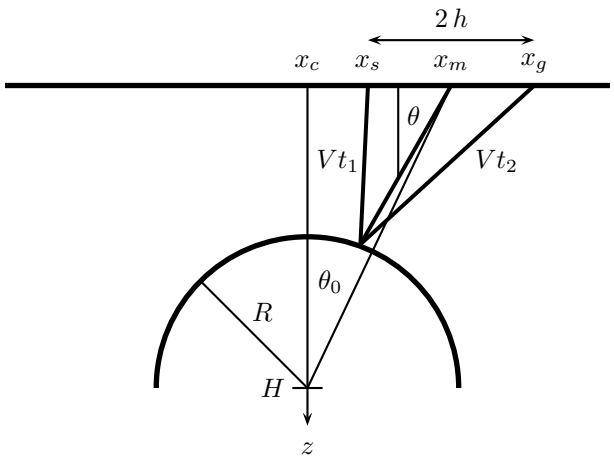

Figure 2: Reflection from a circle with radius R and centre (x_c, H). Traveltimes t_1 and t_2 are those from the stationary point on the circle to the source ($x_s = x_m - x_c - h$) and receiver ($x_g = x_m - x_c + h$), respectively. The angle θ_0 is that between the midpoint and the centre, whereas θ is the angle made by the vertical axis and the line connecting the midpoint and the reflection point.

THE NEW IMPLICIT STACKING OPERATOR

We derive the new stacking operator by considering a spherical reflector with radius R and centre at (x_c, H) (see Figure 2). These quantities can be also expressed in terms of the CRS parameters β_0, R_N, R_{NIP}. The sum t of the traveltimes t_1 and t_2 of the down- and up-going rays with

$$\begin{aligned} V_0^2 t_1^2 &= ((x_m - x_c) - h - R\sin\theta)^2 + (H - R\cos\theta)^2 \\ V_0^2 t_2^2 &= ((x_m - x_c) + h - R\sin\theta)^2 + (H - R\cos\theta)^2 \end{aligned} \tag{5}$$

must fulfil Snell's law in order to describe a reflection from the sphere. This requires that

$$V_0^2 \frac{\partial t}{\partial \theta} = \left(\frac{1}{t_1} + \frac{1}{t_2}\right)(R\,H\sin\theta - R\,(x_m - x_c)\cos\theta) + \left(\frac{1}{t_1} - \frac{1}{t_2}\right) R\,h\cos\theta \quad = \quad 0 \quad . \tag{6}$$

For the zero-offset case, i.e., $h = 0$, we obtain the angle θ_0 from (6) by

$$\tan\theta_0 = \frac{x_m - x_c}{H} \quad . \tag{7}$$

After some algebra, substituting (7) and the identities

$$\begin{aligned} \sin\theta &= \cos\theta_0 \sin(\theta - \theta_0) + \sin\theta_0 \cos(\theta - \theta_0) \\ \cos\theta &= \cos\theta_0 \cos(\theta - \theta_0) - \sin\theta_0 \sin(\theta - \theta_0) \end{aligned} \tag{8}$$

in (6) for $h \neq 0$ leads to

$$\begin{aligned} V_0^2 \frac{\partial t}{\partial \theta} &= R\left(\frac{1}{t_1} + \frac{1}{t_2}\right)\sin(\theta - \theta_0)\sqrt{(x_m - x_c)^2 + H^2} \\ &+ R\left(\frac{1}{t_1} - \frac{1}{t_2}\right)\left\{\cos(\theta - \theta_0)\frac{H\,h}{\sqrt{(x_m - x_c)^2 + H^2}} - \sin(\theta - \theta_0)\frac{h\,(x_m - x_c)}{\sqrt{(x_m - x_c)^2 + H^2}}\right\} \\ &= 0 \quad . \end{aligned} \tag{9}$$

This expression can be solved for

$$\tan(\theta - \theta_0) = \frac{h\,H\,(t_2 - t_1)}{h\,(x_m - x_c)\,(t_2 - t_1) - ((x_m - x_c)^2 + H^2)\,(t_2 + t_1)} \quad . \tag{10}$$

Note that Equation (10) is exact. Since the traveltimes t_1 and t_2 also depend on θ, it cannot be solved analytically. However, if we substitute t_1 and t_2 for the zero-offset case, i.e., $\theta = \theta_0$, in (10), we obtain an update for θ, and thus for the reflection traveltime following (5). Although we could repeat this step in an iterative fashion, we show in the next section that single, direct application of (10) already leads to a higher accuracy than the CRS and planar multifocusing expressions.

EXAMPLES

We have computed traveltime surfaces for four different spherical reflectors with the CRS, planar multifocusing (MF), and the new implicit stacking operator (ISO) expressions. The results were compared with the exact solution. In all cases, we chose V_0=2 km/s, β=0 and R_{NIP}=1 km, and only the radius of the sphere was varied from R=10 m, corresponding to a diffractor-like structure, to R=10 km, describing an almost plane reflector.

The RMS errors compared in Figure 3 were computed for two different apertures: the first one, (a), includes x_m in [-2 km:2 km] and h in [0:1 km], which is equivalent to a maximum offset over reflector depth ratio of two. The second aperture, shown in (b), covering x_m in [-5 km:5 km] and h in [0:2.5 km] was chosen in order to evaluate the accuracy far outside the usually-applied range. Figures 4–6 display the error distributions of the traveltime operators for the different reflector curvatures.

In Figure 3 as well as in Figures 4–6, we observe that within a realistic midpoint and offset range, all three methods perform reasonably well. The accuracy of the CRS expression deteriorates for smaller radii, i.e. toward the diffraction limit. Surprisingly, because this is counter-intuitive, MF is very accurate for diffractions despite the assumption of a planar focusing parameter, and shows higher errors for larger radii. ISO maintains its overall higher accuracy both in the diffraction as in the planar reflection limit over a wide range of midpoints and offsets.

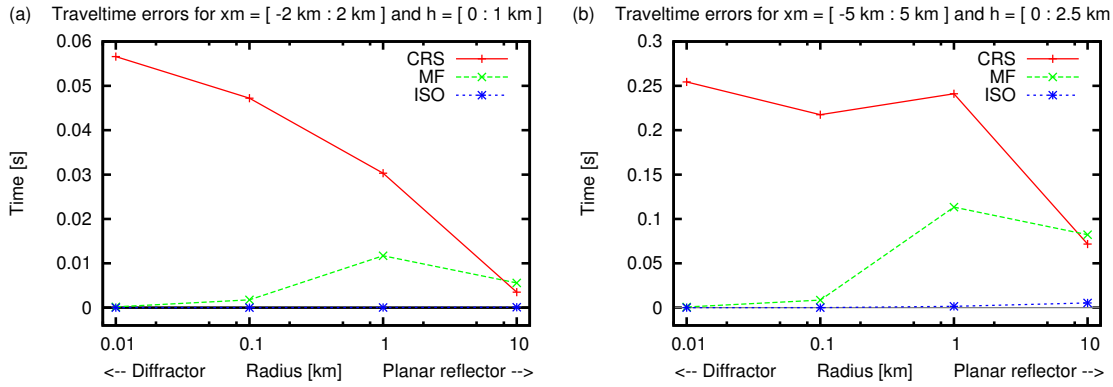

Figure 3: RMS traveltime errors for spherical reflectors with different radii for an aperture of (a) x_m in [-2 km:2 km] and h in [0:1 km], and (b) x_m in [-5 km:5 km] and h in [0:2.5 km]. For both apertures, we observe that the accuracy of CRS deteriorates for smaller radii, i.e. toward the diffraction limit. Planar MF is highly accurate for diffractions, but less so for larger radii. ISO maintains its high accuracy both in the diffraction as well as in the planar reflection limit.

CONCLUSIONS AND OUTLOOK

We have introduced a new implicit stacking operator for curved subsurface structures. Numerical examples show that whereas existing approaches (CRS, planar multifocusing) lead to reasonable accuracy if applied within a realistic midpoint and offset range, the new operator is not only superior to these approaches for larger offsets and midpoint distances, but it also maintains the high accuracy for a wide range of reflector curvatures, from the diffraction limit to quasi-plane reflectors.

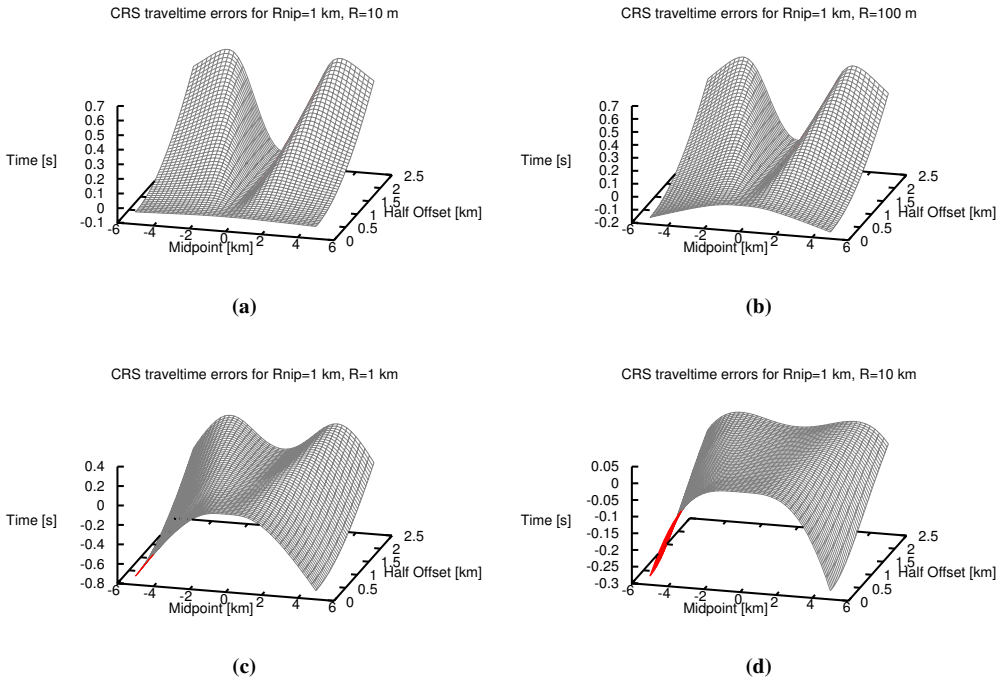

Figure 4: Traveltime errors for the CRS operator for spherical reflectors with (a) R=10 m, (b) R=100 m, (c) R=1 km, (d) R=10 km. The errors decrease for larger radii. Note the different scales.

Future work will include the extension of the new method to three-dimensional subsurface structures and the application to field data.

ACKNOWLEDGEMENTS

We thank the members of the Applied Geophysics Group Hamburg for continuous discussions. Special thanks go to Evgeny Landa from OPERA for providing the multifocusing software. This work was partially supported by the University of Hamburg and the sponsors of the WIT consortium.

REFERENCES

de Bazelaire, E. (1988). Normal moveout revisited – inhomogeneous media and curved interfaces. *Geophysics*, 52:143–157.

Dümmong, S., Baykulov, M., and Gajewski, D. (2009). A workflow for the processing of reflection seismic data with CRS attributes. *SEG, Expanded Abstracts*, 28:3173–3177.

Dümmong, S. and Gajewski, D. (2008). A multiple suppression method via CRS attributes. *SEG, Expanded Abstracts*, 27:2531–2535.

Duveneck, E. (2004). Velocity model estimation with data-driven wavefront attributes. *Geophysics*, 69:265–274.

Gelchinksy, B., Berkovitch, A., and Keydar, S. (1999). Multifocusing homeomorphic imaging – part 1. Basic concepts and formulae. *Journal of Applied Geophysics*, 42:229–242.

Landa, E., Keydar, S., and Moser, T. J. (2010). Multifocusing revisited – inhomogeneous media and curved interfaces. *Geophysical Prospecting*, 1–14:doi: 10.1111/j.1365–2478.2010.00865.x.

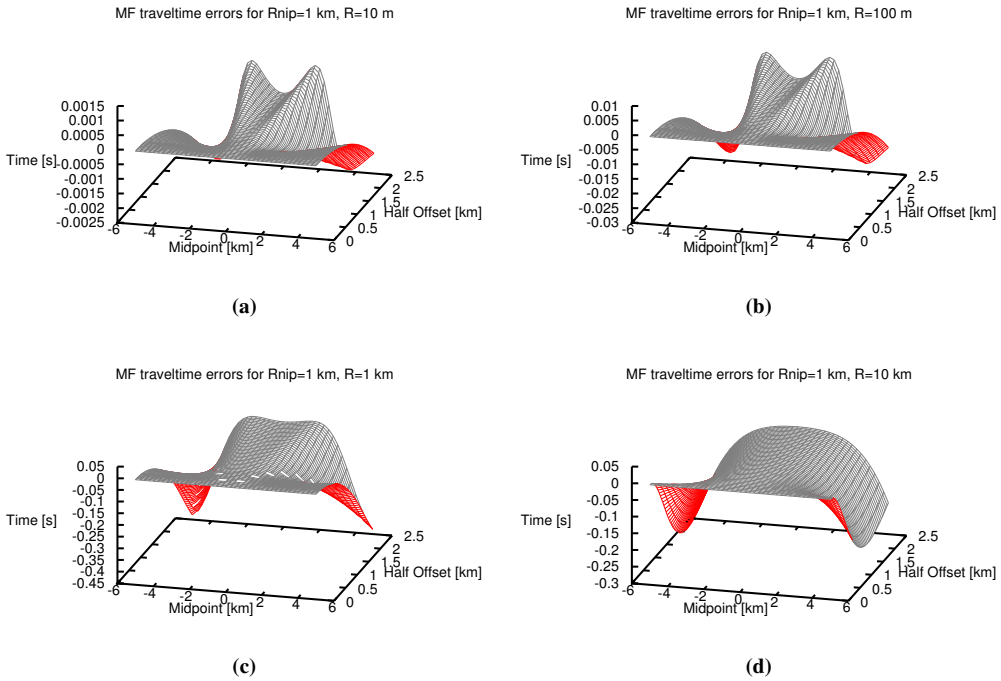

Figure 5: Traveltime errors for the planar MF operator for spherical reflectors with (a) R=10 m, (b) R=100 m, (c) R=1 km, (d) R=10 km. The errors increase for larger radii. Note the different scales.

Mann, J. (2002). *Extensions and Applications of the Common-Reflection-Surface Stack Method*. PhD thesis, University of Karlsruhe.

Mueller, T. (1999). *The Common Reflection Surface stack method – seismic imaging without explicit knowledge of the velocity model*. PhD thesis, University of Karlsruhe.

Müller, N. A. (2007). *Determination of interval velocities by inversion of kinematic 3D wavefield attributes*. PhD thesis, University of Karlsruhe.

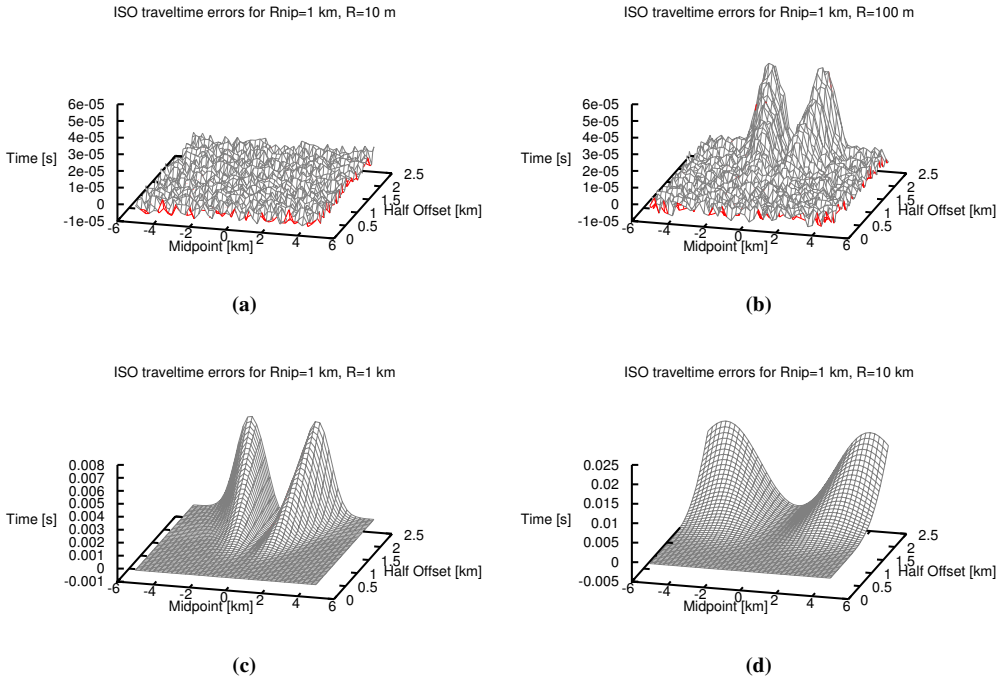

Figure 6: Traveltime errors for the ISO operator for spherical reflectors with (a) R=10 m, (b) R=100 m, (c) R=1 km, (d) R=10 km. The errors increase very mildly for larger radii. For the diffraction limit, errors are within machine precision. Note the different scales.